2014 RISP International Workshop on Nonlinear Circuits,
Communications and Signal Processing
NCSP'14, Honolulu, Hawaii, USA, February 28 - March 3, 2014

Propagation of Frustration in Three Coupled Oscillators as a Ring Topology

Yoko Uwate†, Yosifhimi Nishio† and Ruedi Stoop‡

†Tokushima University
2-1 Minami-Josanjima, Tokushima, Japan
Phone:+81-88-656-7470
Email: {uwate, nishio}@ee.tokushima-u.ac.jp

‡Institute of Neuroinfomatics, UZH/ETH Zurich,
Winterthurerstrasse 190,
CH-8057 Zurich, Switzerland,
Email: ruedi@ini.phys.ethz.ch

Abstract

This paper considers frustration mechanism of three coupled van der Pol oscillators. By using a parallel circuit composed of a resistor and a capacitor as a coupling element, the dynamical behavior of frustration can be observed. We confirm that the propagation speed of frustration differs by the initial conditions.

1. Introduction

Coupled oscillatory systems are good models to express essential role of high-dimensional nonlinear phenomena occurring in the field of natural sciences. Therefore, studies of synchronization phenomena have been extensively reported in physical, biological and electrical systems. Moreover, coupled oscillatory systems can also produce interesting phase patterns, including wave propagation, clustering and complex patterns [1], [2].

In our previous study, our research group have reported interesting synchronization phenomena observed from several types of the oscillatory systems with frustration [3]-[5]. Here, we call frustration which can produce different synchronization state from original system. Frustration can be occurred by network structure, parameter mismatch and so on.

In this study, we consider that the dynamic behavior of frustration can be observed by using a inductor or a capacitor in the coupling element. As a first step, we set the parallel circuit composed of a capacitor and a resistor up as the coupling element. By using a parallel circuit composed of a resistor and a capacitor as the coupling elements, we expect that the dynamical behavior of frustration in the coupling term can be observed.

2. Circuit Model

The circuit model of three coupled van der Pol oscillator as ring topology is shown in Fig. 1. In this circuit model, the network structure is changed by the switch. The adjacent oscillators are coupled by the parallel circuit composed of a resistor and a capacitor. By using this coupling method, the adjacent oscillators tend to synchronize with anti-phase state. The conceptual circuit model and switching operation are shown in Fig. 2. At the beginning, the switch is opened. When the count of Runge-Kutta simulation reaches to 500, 000, the switch is closed. When the switch is off, the adjacent oscillators tend to synchronize with anti-phase state. In this case, the coupled oscillators have no frustration because the energy of the coupling term is zero. While, in the case of that the switch is on, 3-phase synchronization can be observed.

In order to make clear the frustration mechanism, we investigate how to change the synchronization from anti-phase to 3-phase state by measuring the capacitance voltage of the coupling term.

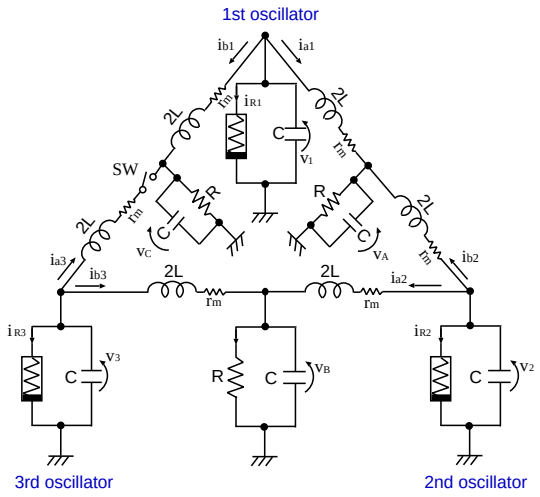

Figure 1: Three coupled van der Pol oscillators as a ring topology.

In the computer simulations, we assume that the $v_k - i_{Rk}$ characteristics of the nonlinear resistor in each oscillator is given by the following third order polynomial equation

$$i_{Rk} = -g_1 v_k + g_3 {v_k}^3 \quad (g_1, g_3 > 0), \quad (k = 1, 2, 3). \tag{1}$$

The normalized circuit equations (SW:ON) governing the circuit in Fig. 1 are expressed as
[First oscillator]

$$\begin{cases} \dfrac{dx_1}{d\tau} = \varepsilon\left(1 - \dfrac{1}{3}{x_1}^2\right)x_1 - (y_{a1} + y_{b1}) \\ \dfrac{dy_{a1}}{d\tau} = \dfrac{1}{2}\left\{x_1 - \eta y_{a1} - x_A\right\} \\ \dfrac{dy_{b1}}{d\tau} = \dfrac{1}{2}\left\{x_1 - \eta y_{b1} - x_C\right\} \end{cases} \tag{2}$$

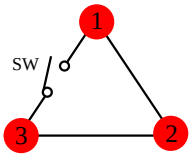

(a) Conceptual circuit model with switch.

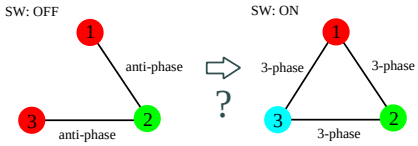

(b) Synchronization and switching operation.

Figure 2: Conceptual circuit model.

[Second oscillator]

$$\begin{cases} \dfrac{dx_2}{d\tau} = \varepsilon\left(1 - \dfrac{1}{3}{x_2}^2\right)x_2 - (y_{a2} + y_{b2}) \\ \dfrac{dy_{a2}}{d\tau} = \dfrac{1}{2}\left\{x_2 - \eta y_{a2} - x_B\right\} \\ \dfrac{dy_{b2}}{d\tau} = \dfrac{1}{2}\left\{x_2 - \eta y_{b2} - x_A\right\} \end{cases} \tag{3}$$

[Third oscillator]

$$\begin{cases} \dfrac{dx_3}{d\tau} = \varepsilon\left(1 - \dfrac{1}{3}{x_3}^2\right)x_3 - (y_{a3} + y_{b3}) \\ \dfrac{dy_{a3}}{d\tau} = \dfrac{1}{2}\left\{x_3 - \eta y_{a3} - x_C\right\} \\ \dfrac{dy_{b3}}{d\tau} = \dfrac{1}{2}\left\{x_3 - \eta y_{b3} - x_B\right\} \end{cases} \tag{4}$$

[Coupling terms]

$$\begin{cases} \dfrac{dx_A}{d\tau} = \beta(y_{a1} + y_{b2}) - \alpha\beta x_A \\ \dfrac{dy_B}{d\tau} = \beta(y_{a2} + y_{b3}) - \alpha\beta x_B \\ \dfrac{dy_C}{d\tau} = \beta(y_{a3} + y_{b1}) - \alpha\beta x_C \end{cases} \tag{5}$$

where

$$t = \sqrt{LC}\tau, \quad v_k = \sqrt{\frac{g_1}{3g_3}}\sqrt{\frac{C}{L}}x_k,$$

$$i_{ak} = \sqrt{\frac{g_1}{3g_3}}\sqrt{\frac{C}{L}}y_{ak}, \quad i_{bk} = \sqrt{\frac{g_1}{3g_3}}\sqrt{\frac{C}{L}}y_{bk},$$

$$\varepsilon = g_1\sqrt{\frac{L}{C}}, \quad \eta = r_m\sqrt{\frac{C}{L}}, \quad \alpha = \frac{1}{R}, \quad \beta = \frac{C}{C_0},$$

$$(k = 1, 2, 3).$$

In this equations, α and β correspond the coupling strength and ε denotes the nonlinearity of the oscillators.

3. Synchronization Phenomena ($\alpha = 20.0$ and $\beta = 1.0$)

For the computer simulations, we calculate Eqs. (2)-(5) using a fourth-order Runge-Kutta method with the step size $h = 0.005$. The parameters of this circuit model are setting for $\varepsilon = 0.1$, $\eta = 0.001$, $\alpha = 20.0$ and $\beta = 1.0$.

3.1. Initial Condition: Anti-Phase State

First, we investigate the capacitance voltages of the coupling term when the initial condition of the coupled oscillators is fixed with anti-phase state.

The simulation result is shown in Fig. 3. x_A, x_B and x_C are corresponding on the capacitance voltages of the coupling term. From this result, before the switch is on, the value of x_A, x_B and x_C show zero. This means that the coupled oscillators have no frustration, because the adjacent oscillators are synchronized with anti-phase state. After the switch is on, all capacitance voltages start to oscillate. The capacitance voltage of x_C shows larger voltage than the others. After certain time, three voltages converge to same amplitude. In this case, three voltages are synchronized with 3-phase state as shown in Fig. 4(a). We also confirm same 3-phase synchronization by using circuit experiment (see. Fig. 4(b)). The parameters of the circuit experiment are set to $L = 50[mH]$, $C = 68[nF]$, $C_0 = 68[nF]$ and $R = 50[\Omega]$.

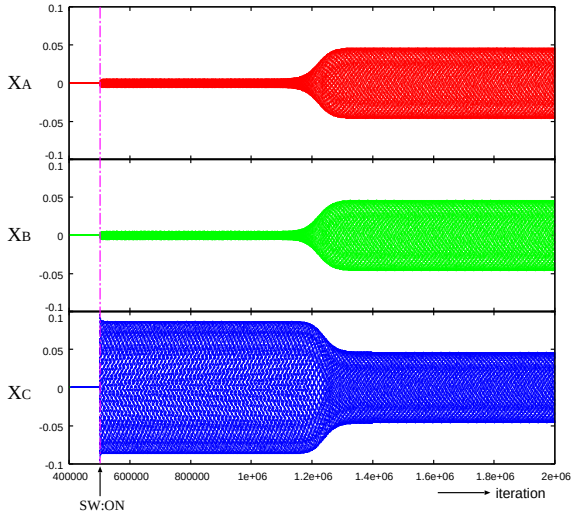

Figure 3: Capacitance voltages of coupling element.

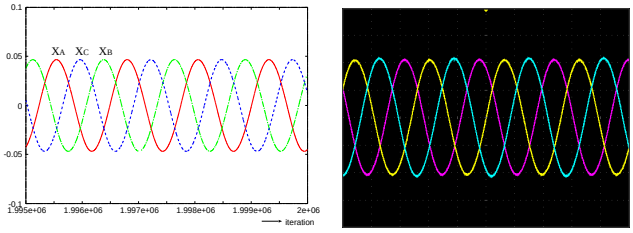

(a) (b)

Figure 4: 3-phase synchronization. (a) Computer simulation. (b) Circuit experiment.

3.2. Initial Condition: In-Phase State

Next, we investigate the capacitance voltages of the coupling term when the initial condition of the coupled oscilla-

tors is fixed with in-phase state.

We observe similar result of the capacitance voltages with above section. However, we find the difference of the convergence time to 3-phase state between in-phase and anti-phase initial conditions. Figure 5 shows the simulation result of x_A obtained from different initial conditions. We confirm that the convergence time of in-phase initial condition is shorter than anti-phase initial condition.

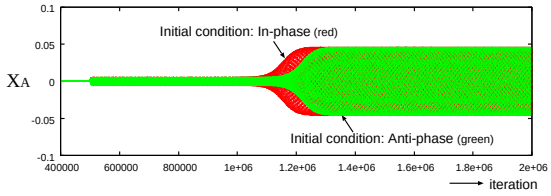

Figure 5: Comparison of capacitance voltages depending on initial conditions (x_A).

We count the convergence time from iteration=500,000 (SW:ON) to 3-phase synchronization (see. Fig. 6). Table 1 summarizes the convergence times of in-phase and anti-phase initial conditions. Two convergence times are difference and T_c of in-phase initial condition is shorter than the anti-phase initial condition.

From this result, we consider that the convergence time could be depending on the past synchronization state. Figure 7 shows the phase differences obtained from in-phase and anti-phase initial conditions. Before the switch is closed, two phase differences show the different synchronization states. In the case of in-phase initial condition, the phase difference changes from 0 to 180 degrees. While, in the case of anti-phase initial condition, the phase difference shows 180 degrees from the beginning.

We assume that the propagation speed of the frustration is depending on the time of the stable synchronization state. Namely, by using the convergence time, we can expect the past synchronization state.

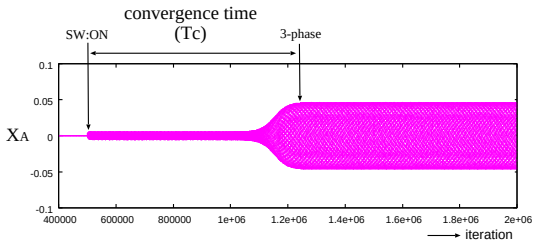

Figure 6: Definition of convergence time (T_c).

Table 1: Convergence time (T_c).

Initial condition	Convergence time (T_c)
In-phase	720,453
Anti-phase	787,824

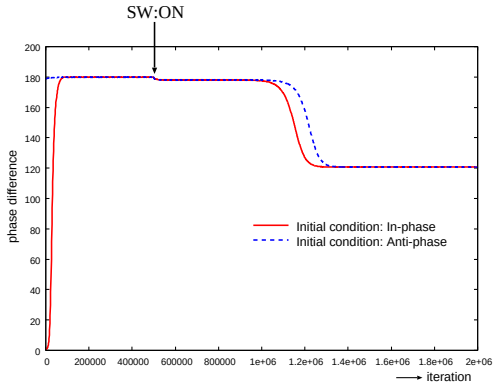

Figure 7: Phase differences (α=20).

4. Parameter Dependency (α and β)

Finally, the parameter dependency of the circuit model is investigated. In this study, we change the parameters of the coupling strength (α and β). α and β correspond to the resistance and capacitance of the parallel circuit of the coupling element.

4.1. Dependence on α

Figure 8 shows the convergence time with α when the initial condition is set to in-phase and anti-phase states. In the both cases, the convergence time has peak around α=10. By increasing α, the convergence time of in-phase initial condition decrease gradually. In the case of anti-phase initial condition, the convergence time also decrease after the peak. While, when α is larger than 20, the convergence time of anti-phase initial condition increases linearly.

Figure 9 shows the phase differences obtained from in-phase and anti-phase initial conditions. In the both cases, the phase difference of in-phase initial condition converges faster than anti-phase initial condition.

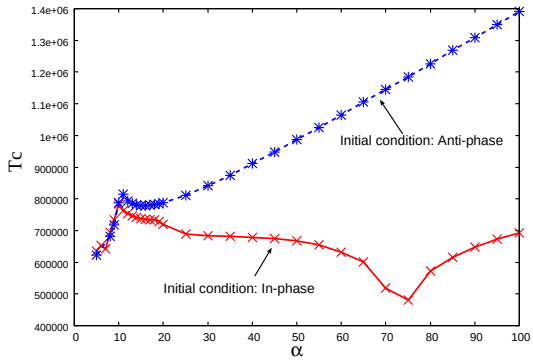

Figure 8: Convergence time depending on α.

In our past study, we have used the amplitude as the frustration evaluation. Figure 10 shows the amplitude value obtained from in-phase and anti-phase initial conditions when α is changed. From this figure, we can see that two lines of the

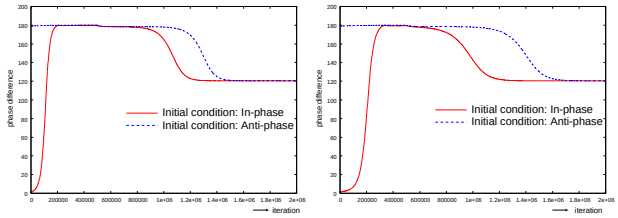

(a) α=40. (b) α=60.

Figure 9: Phase differences.

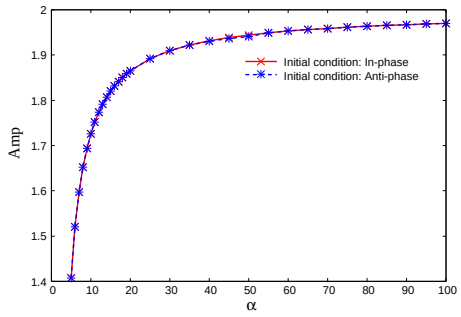

Figure 10: Amplitude depending on α.

amplitudes are completely same. Namely, we consider that the convergence speed of frustration will be used for evaluation of frustration in the coupled oscillatory systems.

4.2. Dependence on β

Figure 11 shows the convergence time with α when the initial condition is set to in-phase and anti-phase states. In the both cases, the convergence time increases when β is smaller than 0.5. By increasing β, the convergence time of the both cases have no change.

Figure 12 shows the amplitude value obtained from in-phase and anti-phase initial conditions when β is changed. We can also see that two lines of the amplitudes are completely same.

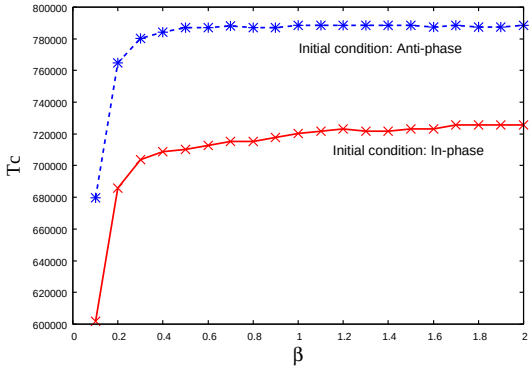

Figure 11: Convergence time depending on β.

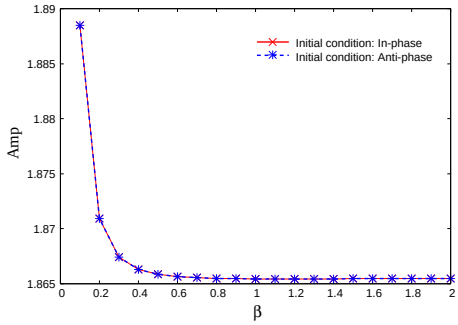

Figure 12: Amplitude depending on β.

5. Conclusions

In this study, we have investigated synchronization phenomena of ring oscillators coupled by a parallel circuit composed of a resistor and a capacitor. By using such coupling elements, we observed interesting frustration mechanism depending on the initial conditions.

The convergence times of in-phase initial condition is shorter than the anti-phase initial condition. Namely, the convergence time could be depending on the past synchronization state. We assume that the propagation speed of the frustration is depending on the time of the stable synchronization state. By using the convergence time, we can expect the past synchronization state.

In the future works, we would like to investigate frustration mechanism of more complex oscillatory systems by using passive device in the coupling elements.

Acknowledgment

This work was partly supported by JSPS Grant-in-Aid for Young Scientists 23700269.

References

[1] M. Yamauchi, M. Wada, Y. Nishio and A. Ushida, "Wave Propagation Phenomena of Phase States in Oscillators Coupled by Inductors as a Ladder," IEICE Trans. Fundam., vol. E82-A, no. 11, pp. 2592-2598, Nov. 1999.

[2] M. Yamauchi, Y. Nishio and A. Ushida, "Phase-waves in a Ladder of Oscillators," IEICE Trans. Fundam., vol. E86-A, no. 4, pp. 891-899, Apr. 2003.

[3] Y. Setou, Y. Nishio and A. Ushida, "Synchronization Phenomena in Many Oscillators Coupled by Resistors as a Ring," *Proc. of APCCAS'94*, pp. 570-575, Dec. 1994.

[4] T. Nagai, Y. Uwate and Y. Nishio, "Rotation of Phase Difference in Four Coupled Oscillators as a Regular Tetrahedron Form," *Proc. of ECCTD'11*, pp. 762-765, Aug. 2011.

[5] Y. Uwate and Y. Nishio, "Synchronization in Several Types of Coupled Polygonal Oscillatory Networks," IEEE TCAS-I, vol. 59, no. 5, pp. 1042-1050, May 2012.